Chemical Engineering Journal 94 (2003) 199–209

Chemical Engineering Journal

www.elsevier.com/locate/cej

Concentration-dependent surface diffusivity model (CDSDM): numerical development and application

Xiaoyan Yang [a,*], Stephen Robert Otto [b], Bushra Al-Duri [a]

[a] *School of Chemical Engineering, The University of Birmingham, Birmingham B15 2TT, UK*
[b] *School of Mathematics and Statistics, The University of Birmingham, Birmingham B15 2TT, UK*

Accepted 23 September 2002

Abstract

In this paper, the film-solid diffusion model (FSDM) combined with a concentration-dependent surface diffusivity $D_s = D_0 \exp\{k(q/q_{sat})\}$ was presented to describe the kinetics of adsorption of reactive dye from aqueous solution onto activated carbon in a batch reactor. A finite-difference scheme was employed to solve the partial differential equations which govern the entire adsorption process in the batch reactor and the resulting kinetic data was presented in terms of the concentration decay curve. It was found that, for the investigated adsorption system, one set of mass transfer parameters was adequate to describe the adsorption rate at different initial solute concentrations. Compared with the constant surface diffusivity model (CSDM), the concentration-dependent surface diffusivity model (CDSDM) yielded a steeper solid-phase concentration profile due to the concentration dependence of D_s. Parametric sensitivity analysis was also carried out in order to facilitate understanding of the effect of each parameter on the shape of the concentration decay curve.

Keywords: Adsorption; Concentration-dependent surface diffusivity model; Kinetics; Mass transfer; Numerical solution; Finite difference

1. Introduction

1.1. The problem considered

The film-solid diffusion model (FSDM) is widely used to describe the adsorption of aqueous solutions by activated carbon [1–3]. FSDM assumes a constant surface diffusivity D_s throughout the entire process of an adsorption operation. However, the thus-obtained D_s has been found to be strongly dependent on either the adsorbed phase concentration corresponding to the initial aqueous concentration or the adsorbed phase concentration at equilibrium, in both single [4] and multi-component systems [3]. This implies that the surface diffusivity changes with the adsorbed phase concentration throughout the entire process of an adsorption operation, which is not reflected by the FSDM. In order to simulate the adsorption process more accurately, it is necessary to incorporate a concentration-dependent surface diffusivity into the FSDM.

Different modelling approaches to the dependence of surface diffusivity on concentration are available. Some of them were reviewed by Kapoor et al. [5]. In the following paragraphs, the most commonly used modelling methods are explained and compared, for the purpose of selecting the suitable concentration-dependent surface diffusivity model (CDSDM) which would be incorporated into the FSDM in this work.

1.1.1. The Arrhenius equation

As for chemical reaction, the Arrhenius equation, when applied to the activation process of surface diffusion, constituted a fundamental requirement for the study of temperature dependence of D_s [5,6]:

$$D_s = D_{s0} \exp\left(-\frac{E_s}{R_g T}\right) \quad (1)$$

where D_{s0} (cm^2/s) is the frequency factor or pre-exponential factor of the surface diffusion at zero surface coverage, E_s (kJ/mol) the activation energy of surface diffusion process, R_g (kJ/(mol K)) the ideal gas constant and T (K) is the temperature. However, Eq. (1) can also be used to study the concentration dependence of D_s via the activation energy of surface diffusion, E_s.

* Corresponding author. Present address: Department of Mechanical and Chemical Engineering, Heriot-Watt University, Edinburgh EH14 4AS, UK. Tel.: +44-131-449-5111-4737; fax: +44-131-451-3129.
E-mail address: x.yang@hw.ac.uk (X. Yang).

1385-8947/03/$ – see front matter
doi:10.1016/S1385-8947(03)00051-2

Nomenclature

a_s	Fritz–Schlünder isotherm parameter $(mg/l)^{-b2}$
$b1$, $b2$	Fritz–Schlünder isotherm parameters
Bi	Biot number $(k_f R C_0/(\rho_s D_0 q_0))$
C	liquid-phase concentration (mg/l)
C_0	initial liquid-phase concentration (mg/l)
C_s	liquid-phase concentration at outer surface of carbon particles (mg/l)
D_0	surface diffusivity at zero surface coverage (cm^2/s)
D_s	surface diffusivity (cm^2/s)
D_{s0}	frequency factor of the surface diffusion at zero surface coverage (cm^2/s)
DC	dimensionless liquid-phase concentration
E	dimensionless quantities $(1/a_s C_0^{b2})$
E_s	activation energy (kJ/mol)
ΔH_{st}	isosteric heat of adsorption (kJ/mol)
k	parameter defined in Eq. (4)
k_f	external liquid film mass transfer coefficient (cm/s)
k_s	Fritz–Schlünder isotherm parameter $(mg/g)(mg/l)^{-b1}$
K	dimensionless quantity (kq_0/q_{sat})
q	solid-phase concentration (mg/g)
q_0	solid-phase concentration in equilibrium with C_0
q_s	solid-phase concentration at outer surface of carbon particles (mg/g)
q_{sat}	solid-phase concentration at surface saturation
Q	dimensionless solid-phase concentration (q/q_0)
r	radial position inside the particle (cm)
R	adsorbent particle radius (cm)
R_g	ideal gas constant (kJ/(mol K))
S	separation factor $(3Wq_0/(VC_0))$
t	time (s)
T	temperature (K)
V	liquid-phase volume (l)
W	mass of activated carbon (g)

Greek letters

τ	dimensionless time $(D_0 t/R^2)$
ρ	dimensionless radial position inside the particle (r/R)
ρ_s	carbon particle density (g/cm^3)

Gilliland et al. [7] correlated E_s with the heat of adsorption $(-\Delta H_{st})$ (kJ/mol) by introducing a proportionality constant ϕ, so that $E_s = \phi(-\Delta H_{st})$. They also indicated that the concentration dependence of D_s could be attributed to the change in the heat of adsorption $(-\Delta H_{st})$ due in turn to the change in surface loading q (mg/g). Neretnieks [8] further assumed a linear relationship between ΔH_{st} and q at constant temperature, and obtained the following equation:

$$D_s = D_0 \exp\left\{k\left(\frac{q}{q_{sat}}\right)\right\} \quad (2)$$

where

$$D_0 = D_{s0} \exp\left(\frac{\phi \Delta H_0}{R_g T}\right) \quad (3)$$

$$k = \frac{\phi(\Delta H_{sat} - \Delta H_0)}{R_g T} \quad (4)$$

ΔH_0 is the enthalpy change of adsorption at $q = 0$, and ΔH_{sat} the enthalpy change of adsorption at saturated state $q = q_{sat}$.

The conversion of Eq. (1) to Eq. (2) has two effects: (i) changing the explicit temperature dependence of D_s to an implicit one and (ii) changing the implicit concentration dependence of D_s to an explicit one. In Eq. (2), the dependence of D_s on temperature is hidden in the expressions of D_0 and k. At constant temperature, it is expected that the surface diffusivities can be correlated with the solid-phase concentrations by using a unique pair of D_0 and k.

Eq. (2) proved to be effective in describing the relationship between D_s and q corresponding to the initial solute concentration or to the equilibrium solute concentration in chlorophenol/activated carbon [4] and dye/activated carbon [3] systems.

1.1.2. Higashi-Ito-Oishi (HIO) model

Based on a random walk of molecules from adsorption site to adsorption site on the solid surface, Higashi et al. [9] proposed the HIO model, as represented by Eq. (5), to correlate D_s directly with the fractional surface coverage θ:

$$D_s = \frac{D_0}{1-\theta} \quad (5)$$

Kapoor and Yang [10] combined Eq. (5) with the pore and surface diffusion model, and compared the result with that from the same model at constant surface diffusivity. They found that employing the concentration-dependent surface diffusivity yielded a higher rate of uptake during adsorption. Hu et al. [11] compared the surface diffusivities derived from the adsorption study of benzene in ink-bottle-like MCM-41 with the HIO prediction. Fair agreement between the two at 298 K was observed.

1.1.3. Chemical potential driving force approach

The chemical potential driving force of adsorption has also been used to derive the concentration dependence of D_s [6,12]. According to this approach, D_s at a certain amount adsorbed, can be expressed on the basis of the surface diffusivity at zero surface coverage, D_0, as follows:

$$D_s = D_0\left(\frac{\mathrm{d}\ln c}{\mathrm{d}\ln q}\right) \quad (6)$$

where c is the gas/liquid-phase concentration in equilibrium with the solid-phase concentration, q.

In Eqs. (5) and (6), the temperature dependence of D_s is hidden in D_0, which in turn, can be expressed by the Arrhenius equation, as follows:

$$D_0 = D_{s0} \exp\left(\frac{-E_{s0}}{R_g T}\right) \tag{7}$$

where E_{s0} is the activation energy of adsorption at $q = 0$.

Miyabe and Takeuchi [6] proposed a restricted molecular diffusion model (RMDM) for the activation process of surface diffusion, on the basis of the two-step theory postulated by Komiyama and Smith [13]. According to the RMDM, the surface diffusivity at zero surface coverage of an adsorbate, D_0, can be derived as follows:

$$D_0 = D_{s0} \exp\left\{\frac{-(E_m + \phi(-\Delta H_{st}))}{R_g T}\right\} \tag{8}$$

where E_m (kJ/mol) is the activation energy of molecular diffusion of the adsorbate.

Theoretically, ΔH_{st} in Eq. (8) is the enthalpy change of adsorption at $q = 0$, it should be independent of the change in solid-phase concentration q during the adsorption process. However, Miyabe and Takeuchi [6] neglected the fact and regarded ΔH_{st} in Eq. (8) as corresponding to a certain amount adsorbed, q ($0 \le q \le q_{sat}$). They also correlated ΔH_{st} with q_{st}, the isosteric heat of adsorption corresponding to the saturated concentration of the adsorbate in the bulk phase and, the adsorption potential E_{ap} (kJ/mol) which changes with q:

$$\Delta H_{st} = q_{st} - E_{ap} \tag{9}$$

By combining Eqs. (6), (8) and (9):

$$D_s(q, T) = D_{s0}\left(\frac{\mathrm{d}\ln c}{\mathrm{d}\ln q}\right) \exp\left\{\frac{-(E_m + \beta(-q_{st} + E_{ap}))}{R_g T}\right\} \tag{10}$$

Eq. (10) was applied to the analysis of surface diffusion phenomena in various adsorption systems and it provided a consistent explanation of the dependence of D_s on both temperature and the amount adsorbed [6].

1.1.4. Comparison of the concentration-dependent surface diffusivity models

Although Eq. (10) seems to be the most comprehensive expression of the factors which influence D_s, such as temperature, the amount adsorbed, and the adsorptive interaction between adsorbate molecules and the surface of adsorbents, its inherent complexity hinders its usage in complicated mass transfer models. At best, Eq. (10) can be reduced to the following equation when assuming a linear relationship between E_{ap} and q:

$$D_s = D'_{s0}\left(\frac{\mathrm{d}\ln c}{\mathrm{d}\ln q}\right) \exp(k' q) \tag{11}$$

where D'_{s0} and k' are two constants at a prescribed temperature.

Eq. (11) still has a more complex form than Eq. (2). From a numerical point of view, involving Eq. (11) in any complicated mass transfer model will be much more costly than involving Eq. (2) in terms of code development time and computational time. Thus, the advantage of Eq. (11) lies in its ability to interpret experimental results, but not in the numerical prediction of adsorption process.

With regard to Eqs. (5) and (6), Eq. (5) has an intrinsic disadvantage, which is D_s would become infinite at full surface coverage. The application of Eq. (6) is restricted to non-Freündlich-type adsorption, as $(\mathrm{d}\ln c/\mathrm{d}\ln q)$ does not vary in Freündlich-type adsorption, thus the concentration dependence of D_s could not be represented under such circumstances.

Eq. (2) does not have any of the disadvantages mentioned above. Therefore, Eq. (2) was incorporated into the FSDM in this work. In the following discussion, the combination of Eq. (2) and FSDM was called the concentration-dependent surface diffusivity model (CDSDM). In the CDSDM, when assuming $k = 0$ in Eq. (2), D_s would become constant and the CDSDM would simplify to the constant surface diffusivity model (CSDM). Thus, comparison between CDSDM and CSDM predictions can be carried out without extra coding.

It is worth mentioning that CDSDM is superior to other adsorption models which employ a constant surface diffusivity over the entire adsorption process (e.g. the combined pore-surface diffusion model). This is because the latter do not reflect the fact that the value of D_s does not remain constant during an adsorption process but increases continuously with time until equilibrium is reached.

1.2. Outline of the present contribution

Chatzopoulos et al. [14] combined Eq. (2) with the film-solid diffusion model in their study of toluene adsorption on activated carbon, although no analysis of the advantage of Eq. (2) over other models was made. The orthogonal collocation method (OCM) was then employed to solve the partial differential equations. They succeeded in fitting the adsorption rates in a batch reactor under a variety of operating conditions with a single D_0 and k defined in Eq. (2).

In this paper, the film-solid diffusion model incorporating the same variable solid diffusivity was solved with a finite-difference scheme. The advantage of such a scheme and the detailed numerical development of the model are given in Section 3, following the equations presented in Section 2. Features of the batch experiment, which was used to validate the model, are described in Section 4. Results and discussion are contained in Section 5. In Section 6, conclusions are made from the results and discussion.

It should be noted that a reactive dye/activated carbon adsorption system had been selected for the experiment. This was mainly due to the following factors: (i) reactive dyes

are among the most often found components in dyehouse wastewater, and adsorption by activated carbon is commonly used as a finishing step where low concentration of dyes can be removed during dyehouse wastewater treatment [15]. Thus the study of the surface diffusion behaviour of reactive dye on activated carbon has its practical significance; (ii) reactive dye has a much different molecular size and structure from that of toluene. The successful application of the CDSDM to the adsorption of reactive dye will further validate the concentration dependence of surface diffusivity represented by Eq. (2).

2. Theoretical model

According to the FSDM, adsorption would take place by external mass transfer across the boundary layer, followed by surface diffusion to the sorption sites, where adsorbate molecules would be rapidly taken up. Surface diffusion would be assumed to occur by the surface hopping mechanism. Adsorbate molecules would diffuse within the adsorbent particles by surface migration from one site to another on the outer surface and the pore walls. Due to its advantages mentioned in Section 1.1, Eq. (2) was selected and incorporated in the FSDM to represent the concentration dependence of D_s on surface loading q.

The fundamental equations for the kinetics of the adsorption process in a batch reactor are as follows:

(1) Liquid-phase mass balance

$$V\frac{dC}{dt} = -\frac{3W}{\rho_s R}k_f(C - C_s) \tag{12}$$

Initial condition:

$$t = 0, \quad C = C_0 \tag{13}$$

(2) Solute diffusion inside a spherical adsorbent particle

$$\frac{\partial q}{\partial t} = \frac{D_0}{r^2}\frac{\partial}{\partial r}\left[r^2 \exp\left\{k\left(\frac{q}{q_{sat}}\right)\right\}\frac{\partial q}{\partial r}\right] \tag{14}$$

Initial condition:

$$t = 0, \quad 0 \le r \le R, \quad q = 0 \tag{15}$$

Boundary condition:

$$t > 0, \quad \left.\frac{\partial q}{\partial r}\right|_{r=0} = 0 \tag{16}$$

$$D_0\rho_s \exp\left\{k\left(\frac{q}{q_{sat}}\right)\right\}\left.\frac{\partial q}{\partial r}\right|_{r=R} = k_f(C - C_s) \tag{17}$$

(3) Equilibrium at the solid–liquid interphase, which is described by the Fritz–Schlünder isotherm:

$$q_s = \frac{k_s C_s^{b1}}{1 + a_s C_s^{b2}} \tag{18}$$

Using the dimensionless quantities,

$$DC = \frac{C}{C_0}, \quad DC_s = \frac{C_s}{C_0}, \quad Q = \frac{q}{q_0}, \quad Q_{sat} = \frac{q_{sat}}{q_0},$$
$$\rho = \frac{r}{R}, \quad \tau = \frac{D_0 t}{R^2}, \quad Bi = \frac{k_f R C_0}{\rho_s D_0 q_0}, \quad S = \frac{3Wq_0}{VC_0},$$
$$E = \frac{1}{a_s C_0^{b2}}, \quad K = \frac{kq_0}{q_{sat}}$$

Eqs. (12)–(18) can be reduced to the following dimensionless form:

$$\frac{d(DC)}{d\tau} = -S\,Bi(DC - DC_s) \tag{19}$$

$$\tau = 0, \quad DC = 1 \tag{20}$$

$$\frac{\partial Q}{\partial \tau} = \frac{1}{\rho^2}\frac{\partial}{\partial \rho}\left\{\rho^2 \exp(KQ)\frac{\partial Q}{\partial \rho}\right\} \tag{21}$$

$$\tau = 0, \quad 0 \le \rho \le 1, \quad Q = 0 \tag{22}$$

$$\tau > 0, \quad \left.\frac{\partial Q}{\partial \rho}\right|_{\rho=0} = 0 \tag{23}$$

$$\exp(KQ)\left.\frac{\partial Q}{\partial \rho}\right|_{\rho=1} = Bi(DC - DC_s) \tag{24}$$

$$Q_s = \frac{DC_s^{b1}(1 + E)}{DC_s^{b2} + E} \tag{25}$$

3. Development of numerical solution

3.1. Numerical development of the model

Eqs. (19)–(25) cannot be solved analytically. However, a corresponding numerical solution can be obtained by numerical techniques such as orthogonal collocation method (OCM) and finite-difference method (FDM). Chatzopoulos et al. [14] employed the OCM to solve these equations. Nevertheless, OCM is not the best method to solve problems of this type since, for a given choice of Jacobi polynomials, the discretization along the radial direction is determined exclusively by the number of collocation points [16]. Generally speaking, the FDM has two main advantages over the OCM for the problem being investigated: (i) FDM is easier to code than OCM; (ii) the solution of FDM is much more stable than that of OCM.

In both the film-solid diffusion model with a constant D_s [1] and the branched pore kinetic model [17,18], the internal mass transfer rates were expressed in terms of a linear partial differential equation of second order in two independent variables (time t and position r). In the case of the concentration-dependent surface diffusivity model, the partial differential equation Eq. (21) is non-linear. As it is impossible to construct a fully implicit scheme, the problem has to be dealt with using an iterative technique. An initial

guess is made for the solution (usually that from the previous step) and its deviation from the true solution ΔQ is taken to be small. The linearised equations are solved and $Q \rightarrow Q + \Delta Q$. If this new iterate is the true solution then $\Delta Q = 0$ and the solution will have converged, or at least $|\Delta Q/Q| \leq \varepsilon$ for all ρ, where ε is the criterion for convergence of the computation. In this study, ε was set to be equal to 10^{-5}.

The detailed numerical approach for this problem is as follows.

The two-dimensional space (time τ and position ρ) is meshed with time step $\Delta\tau$ and distance step $\Delta\rho$. The grid point is labelled as (n, m) with integer n corresponding to time $n\,\Delta\tau$ ($n \leq 0$) and integer m corresponding to the position $m\,\Delta\rho$ ($0 \leq m \leq M$, $M\,\Delta\rho = 1$). The converged solution Q at time $n\,\Delta\tau$ and position $m\,\Delta\rho$ are denoted as Q_m^n.

Suppose the solution for Q is known at the time level $n\,\Delta\tau$, Q_m^g represents the first approximate to Q_m^{n+1}. As mentioned above, $Q_m^g = Q_m^n$ can be taken or $Q_m^g = Q_m^n + (Q_m^n - Q_m^{n-1})$ can be taken to slightly speed up the convergence. The term ΔQ_m represents the difference between Q_m^{n+1} and Q_m^g, thus

$$Q_m^{n+1} = Q_m^g + \Delta Q_m \tag{26}$$

Applying the forward difference method to Eqs. (19)–(24) for temporal derivatives and introducing Eq. (26) into the same set of equations, the following equation is obtained:

$$\left\{\frac{(\Delta\rho)^2 \exp(-KQ_0^g)}{\Delta\tau} + 2K(Q_1^g - Q_0^g) + 6\right\}\Delta Q_0 - \{2K(Q_1^g - Q_0^g) + 6\}\,\Delta Q_1 = -\exp(-KQ_0^g)\left\{\frac{(\Delta\rho)^2(Q_0^g - Q_0^n)}{\Delta\tau}\right\} + K(Q_1^g - Q_0^g)^2 + 6(Q_1^g - Q_0^g), \quad m = 0 \tag{27}$$

$$-\Delta Q_{m-1} + \left\{\frac{(\Delta\rho)^2}{\Delta\tau}\exp(-KQ_m^g) + \frac{2+2m}{m} + 2K(Q_{m+1}^g - Q_m^g)\right\}\Delta Q_m - \left\{\frac{2+m+2Km(Q_{m+1}^g - Q_m^g)}{m}\right\}\Delta Q_{m+1} = -\exp(-KQ_m^g)(Q_m^g - Q_m^n)\frac{(\Delta\rho)^2}{\Delta\tau} + \frac{2(Q_{m+1}^g - Q_m^g)}{m} + K(Q_{m+1}^g - Q_m^g)^2 + (Q_{m+1}^n - 2Q_m^n + Q_{m-1}^n), \quad 1 \leq m \leq M-1 \tag{28}$$

$$\exp(KQ_M^g)(\Delta Q_M - \Delta Q_{M-1}) = \Delta\rho Bi(\mathrm{DC}^{n+1} - \mathrm{DC}_s^{n+1}) - \exp(KQ_M^g)(Q_M^g - Q_{M-1}^g), \quad m = M \tag{29}$$

Eq. (28) is a general expression derived from Eq. (21) for $1 \leq m \leq M-1$. When $m = 0$, this equation is no longer valid and the condition $\partial Q/\partial\rho|_{\rho=0} = 0$ is thus used and Eq. (27) is derived. Eq. (29) follows directly from Eq. (24).

Applying Crank–Nicolson approach to Eq. (19) yields the following equation:

$$\mathrm{DC}^{n+1} = \frac{(1-\mathrm{SB})\mathrm{DC}^n + \mathrm{SB}(\mathrm{DC}_s^{n+1} + \mathrm{DC}_s^n)}{1+\mathrm{SB}} \quad \text{where} \quad \mathrm{SB} = \frac{S \cdot Bi \cdot \Delta\tau}{2} \tag{30}$$

Eqs. (27)–(30) can be conveniently written in matrix form $A \cdot \overrightarrow{\Delta Q} = \vec{b}$ and then solved iteratively.

3.2. Program outline

A Fortran 90 program has been developed to solve the above problem. First, the program reads the various input data from a data file, secondly, the banded coefficient matrix A is transformed so that it can be factorised using NAG subroutine F07BDF, and then the matrix equation is solved by NAG subroutine F07BEF. There are two main loops in the calculation: (1) first input an estimated vector Q_m^g and an estimated value for $(\mathrm{DC}^{n+1} - \mathrm{DC}_s^{n+1})$. The program will solve the matrix equation iteratively until $|\Delta Q/Q| \leq 10^{-5}$; (2) when (1) is satisfied, the program will calculate DC_s^{n+1} by Eq. (25) and consequently DC^{n+1} by Eq. (30), if the difference between the calculated $(\mathrm{DC}^{n+1} - \mathrm{DC}_s^{n+1})$ and the estimated $(\mathrm{DC}^{n+1} - \mathrm{DC}_s^{n+1})$ is larger than the set requirement, the calculated $(\mathrm{DC}^{n+1} - \mathrm{DC}_s^{n+1})$ will substitute the original one and the computation repeats until the requirement for the difference is satisfied. The program output provides the experimental and theoretical concentration decay curves.

4. Experimental

4.1. Materials

Activated carbon Filtrasorb-400 (F-400) from Calgon Carbon was used as adsorbent for the present work. Reactive Navy (Ciba Geigy), a reactive dye that is frequently used in the textile industry, was selected as adsorbate. Physical properties of this kind of dye are well cited in literature [15,19].

4.2. Equilibrium and kinetics study

Both the equilibrium study and the kinetics study were carried out at 298 K.

Equilibrium study was conducted by bringing a series of aqueous solutions of Reactive Navy into contact with certain amounts of carbon for a long enough time.

The effect of initial concentrations on the adsorption of Reactive Navy onto F-400 was investigated in an agitated tank. Five runs of the experiment were carried out, with the initial dye concentration ranging from 13.2 to 163 mg/l. For each run, the solution volume was 2.5 l, the agitation

speed was maintained constant at 400 rpm, the mass of activated carbon was 7.5 g, and the average particle diameter is 0.0536 cm. A more detailed description of the experiment can be found in [18].

5. Results and discussion

5.1. Equilibrium isotherm

The optimum values of the parameters employed in the Fritz–Schlünder isotherm (Eq. (18)) were obtained by fitting the model prediction to the experimental solid-phase equilibrium concentrations. The thus-obtained parameter values were:

$$k_s = 9.23\,(\text{mg/g})\,(\text{mg/l})^{-b1}, \qquad a_s = 0.180\,(\text{mg/l})^{-b2},$$
$$b1 = 0.717, \qquad b2 = 0.639$$

More information on the equilibrium isotherm can be found in [18].

5.2. Production of the theoretical concentration decay curves

In the CDSDM, there are three major parameters, namely, k_f (cm/s) the external mass transfer coefficient, D_0 (cm^2/s) the surface diffusivity at zero surface loading and k, the parameter defined in Eq. (4). The shape of the theoretical concentration decay curves results from the non-linear combination of the three mass transfer parameters.

As all the runs of the experiment were conducted under the same hydrodynamics condition, and the initial concentration range employed is narrow, it is expected that the respective external mass transfer coefficient k_f for all the runs would be the same. Meanwhile, a pair of D_0 and k is supposed to be able to describe the intraparticle diffusion at any solid-phase concentration. Thus in this paper, one set of the three above mentioned mass transfer parameters should be adequate in describing all the experimental data.

The best-fit values of k_f, D_0 and k were determined by minimising the root mean square of the normalised residuals between the experimental liquid-phase concentration C_{exp} and the model prediction C_{cal} for all experimental data (abbreviated as RMS_A).

$$RMS_A = \sqrt{\frac{\sum_{i=1}^{N_{run}} \sum_{j=1}^{N_{pt,i}} (1 - C_{cal,ij}/C_{exp,ij})^2}{\sum_{i=1}^{N_{run}} N_{pt,i}}} \tag{31}$$

where N_{run} is the number of experimental curves, $N_{pt,i}$ is the number of points on the ith experimental curve. In this work, $N_{run} = 5$ and $N_{pt,i} = 17$ ($i = 1, 2, \ldots N_{run}$).

An effective and easy-to-use NAG subroutine E04JAF has been employed to carry out the searching process. E04JAF requires input of the starting values of the three parameters and their corresponding upper and lower bounds. The starting value of k_f was obtained as follows: at each initial concentration, an external mass transfer coefficient was estimated by the initial slope method [20], as shown in Table 1; the mean value of these estimated external mass transfer coefficients was then taken as the starting value of k_f. For D_0 and k, data from literature [14,18] were used as guideline to decide their starting values. The starting values were then adjusted automatically during curve fitting until a minimum RMS_A value was found.

Table 1
The estimated k_f values at different initial concentrations of Reactive Navy

Initial concentration (mg/l)	Estimated k_f from the initial slope method (cm/s)
13.2	4.9E−4
43.3	3.4E−4
76.1	1.3E−4
106	1.1E−4
163	1.8E−4
Mean value	2.5E−4

For the Reactive Navy/F-400 system, the mass transfer parameters thus obtained were $k_f = 5.0\text{E}{-4}$ cm/s, $D_0 = 1.20\text{E}{-11}$ cm^2/s and $k = 3.0$ with $RMS_A = 4.07\%$. Fig. 1 compares the experimental concentration decay curves with the CDSDM predictions. From Fig. 1 and the low RMS_A value, it can be concluded that the fitting between the experimental data and the model predictions is satisfactory.

Based on the best-fit parameter values for Reactive Navy/F-400 system, the surface diffusivity D_s at surface saturation ($q = q_{sat}$) was about 20 times of the surface diffusivity at $q = 0$, indicating a strong dependence of D_s on surface loading.

In the adsorption of toluene onto F-300 activated carbon [14], the mass transfer coefficient that could best describe adsorption kinetics were found to be $D_0 = 3.59\text{E}{-9}$ cm^2/s, $k = 5.09$.

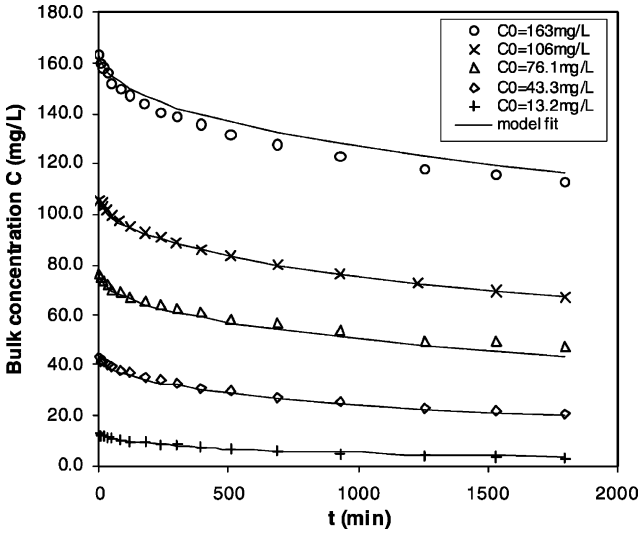

Fig. 1. Experimental rate curves and model fit by CDSDM for Reactive Navy/F-400 system in a batch reactor.

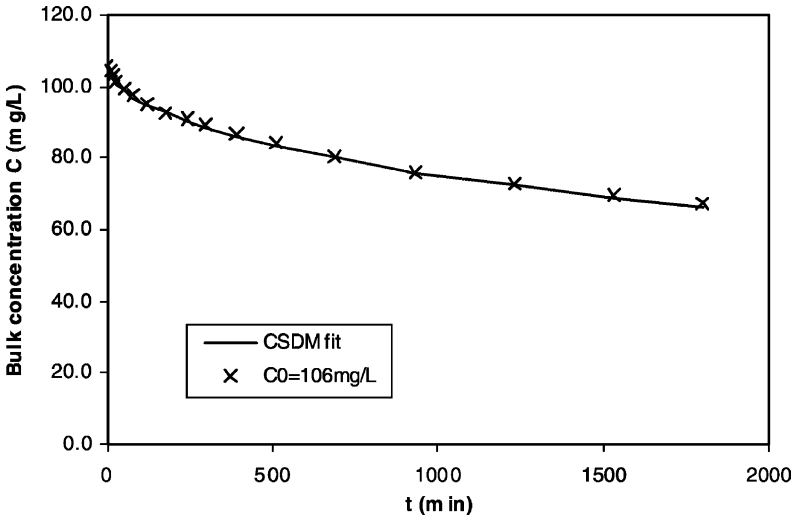

Fig. 2. Experimental rate curve and model fit by CSDM at $k_f = 5.0E{-}4$ cm/s, $D_s = 4.25E{-}11$ cm^2/s.

The larger values of D_0 and k for toluene indicate that toluene is a faster diffuser than Reactive Navy, and its diffusion rate is more sensitive towards changes in solid-phase loading than Reactive Navy. This is expected, as the molecular size and molecular weight of Reactive Navy is much larger than that of toluene. Thus, Reactive Navy possesses bigger inertia, which limits its diffusion and makes it less sensitive towards changes in solid-phase concentration. Also, due to its complex structure, Reactive Navy has a more interactive nature, hence it is more strongly adsorbed and therefore has a slower diffusivity.

The concentration dependence of D_s can be explained by the energetic heterogeneity of the surface or the thermodynamic non-ideality of the amount adsorbed, the increase in the mean free path of surface diffusion with surface loading and the lateral interactions among the adsorbed molecules at high surface coverage [5,14,21]. Among them, the energetic heterogeneity of the surface would be the most important factor.

In adsorption, the surface heterogeneity would mean different adsorption sites hold different amount of adsorption energy. From thermodynamic point of view, the first sites on a surface to be occupied would be those which attract adsorbate molecules most strongly and with the greatest release of energy, then adsorption would take place on those energetically weaker sites [22]. As the surface loading increased, the surface-adsorbate interactions for the newly adsorbed molecules would become gradually weaker, and the activation energy for surface diffusion would decrease, thus these molecules would be able to move more freely on the surface, resulting in a higher surface flux.

5.3. Comparison of CDSDM and CSDM

As mentioned earlier, when the value of k was zero in the CDSDM, the model was reduced to the constant surface diffusivity model. It was noticed that CSDM could yield the same concentration decay curve provided the mass transfer parameters were chosen carefully. Fig. 2 shows the theoretical concentration decay curve for $C_0 = 106$ mg/l by CSDM at $k_f = 5.0E{-}4$ cm/s, $D_s = 4.25E{-}11$ cm^2/s. Good agreement between the experimental data and the model fit can be observed.

However the use of these two mass transfer parameters failed to describe satisfactorily the adsorption rates at other initial solute concentrations, as shown in Table 2 by the root mean square of the normalised residuals between the experimental liquid-phase concentration C_{exp} and the model prediction C_{cal} for a single run of experiment (abbreviated as RMS_S).

$$RMS_S = \sqrt{\frac{1}{N_{pt,i}} \sum_{j=1}^{N_{pt,i}} \left(1 - \frac{C_{cal,ij}}{C_{exp,ij}}\right)^2} \quad (i = 1, 2, \ldots, N_{run}) \tag{32}$$

Despite the consistency between the predicted concentration decay curves at $C_0 = 106$ mg/l by both CDSDM and CSDM, there exists much difference in the solid-phase concentration profile produced by the two models. Fig. 3 compares the solid-phase concentration profile by the two models at time $t = 1799$ min and $t = 5397$ min.

Table 2
RMS_S values corresponding to the fitting by CDSDM and CSDM

Initial concentration (mg/l)	RMS_S (%)	
	CDSDM	CSDM
13.2	7.32	19.7
43.3	2.12	9.45
76.1	4.02	6.22
106	0.812	0.885
163	2.79	3.98

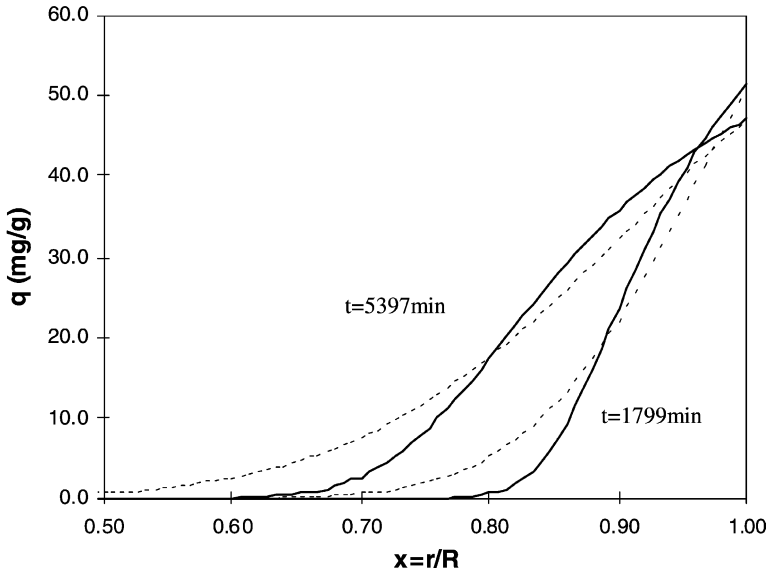

Fig. 3. Comparison of solid-phase concentration profile yielded by different model; CDSDM by solid line. CSDM by dashed line.

It could be observed from Fig. 3 that, near the particle surface, the solid-phase concentration profiles corresponding to the CDSDM were higher than that corresponding to the CSDM, and it was the other way around near the centre of the particle. The similar phenomenon was reported by Kapoor and Yang [10], and it was contributed to the concentration dependence of D_s.

From the mathematical point of view, the shape of q versus r curve at the outer surface of the particle would be determined by the boundary condition there.

In the CDSDM, the boundary condition represented by Eq. (17) can be rewritten as:

$$\left.\frac{\partial q}{\partial r}\right|_{r=R} = \frac{k_f(C - C_s)}{D_0 \rho_s \exp\{k(q/q_{sat})\}_{r=R}} \tag{33}$$

The counterpart of Eq. (33) in CSDM is:

$$\left.\frac{\partial q}{\partial r}\right|_{r=R} = \frac{k_f(C - C_s)}{D_s \rho_s} \tag{34}$$

According to the liquid-phase mass transfer equation represented by Eq. (12), if the two models at their respective mass transfer parameters could produce the same C versus t curves, the value of $k_f(C - C_s)$ for the two models should be equivalent at any time. In the case that k_f are identical, C_s and q_s will also be the same. The values of D_s at the outer surface of adsorbent particle in the CDSDM (given by $D_0 \exp\{k(q/q_{sat})\}$) were calculated to be 6.48E−11 cm^2/s at $t = 1799$ min and 5.63E−11 cm^2/s at $t = 5397$ min. These values were larger than 4.25E−11 cm^2/s, the surface diffusivity value at the outer surface of adsorbent particle in the CSDM. Thus $(\partial q/\partial r)_{r=R}$ corresponding to the CDSDM would be smaller than that corresponding to the CSDM. As $(\partial q/\partial r)_{r=R}$ represented the slope of the solid-phase concentration profile at the outer surface of particle, a smaller $(\partial q/\partial r)_{r=R}$ implied a flatter curve near the outer surface of the particle. Therefore the solid-phase concentration for the CDSDM at the outer surface of the particle is higher than that for the CSDM.

On the other hand, near the centre of the particle, as the solid-phase concentration would be very low, the surface diffusivity $D_s = D_0 \exp\{k(q/q_{sat})\}$ was less than 4.25E−11 cm^2/s, thus the flux in correspondence to the CSDM will be higher than that in correspondence to the CDSDM.

Whether a steeper solid-phase concentration profile is a better representative of the true system is still unclear. The very few researches on experimental observation of the evolution of the surface concentration profile includes that of Spahn and Schlünder [20]. They monitored the adsorption of C^{14}-labelled phenylacetic acid onto activated carbon, and concluded that the solid-phase concentration profile was indeed quite sharp.

Despite inadequate experimental proof of the steep solid-phase concentration profile, CDSDM has succeeded in describing the dependence of surface diffusivity on solid-phase concentrations by one set of mass transfer coefficient (D_0 and k), in both toluene/F-300 system [14] and Reactive Navy/F-400 system. This indicates a promising applicability of CDSDM, as Reactive Navy and toluene are very much dissimilar in terms of molecular size, molecular weight and polarity, etc.

5.4. Parametric sensitivity analysis

Parametric sensitivity analysis is a very useful tool in numerical study. In this work, it can be used to study the effects of various variables on the shapes of the overall concentration decay curve and the intraparticle concentration profile.

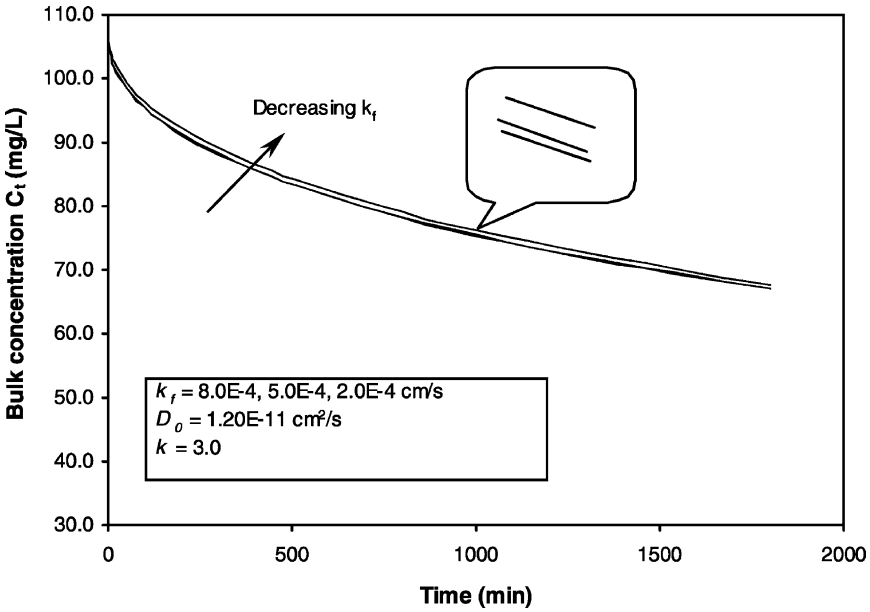

Fig. 4. Parametric sensitivity analysis; effect of k_f on the concentration decay curves.

This has two different significances. First, the parametric sensitivity analysis towards the model parameters can indicate which model parameter affects the concentration decay curve to what extent, and in which way. Such information can be used to decide what is the rate-controlling step; it can also help speed up the curve-fitting process and the determination of the model parameters if the "trial-and-error" method is used to search for the best-fit parameters. Second, the parametric sensitivity analysis towards variables representing the operating conditions (e.g. the initial concentration) can be used to study how these changes affect the adsorption performance.

Parametric sensitivity analysis is normally performed by choosing a standard value for the parameter and then studying the effect caused by changes in the parameter value. In this paper, the standard parameter values employed are those which yielded the best-fit to the experimental data, i.e. $k_f = 5.0\text{E}{-4}$ cm/s, $D_0 = 1.20\text{E}{-11}$ cm^2/s and $k = 3.0$. The sensitivity analysis was then carried out by changing each parameter by ±60%, respectively, while keeping the other two parameters unchanged.

Figs. 4–6 display the patterns in which the concentration decay curves vary with each mass transfer parameter, respectively.

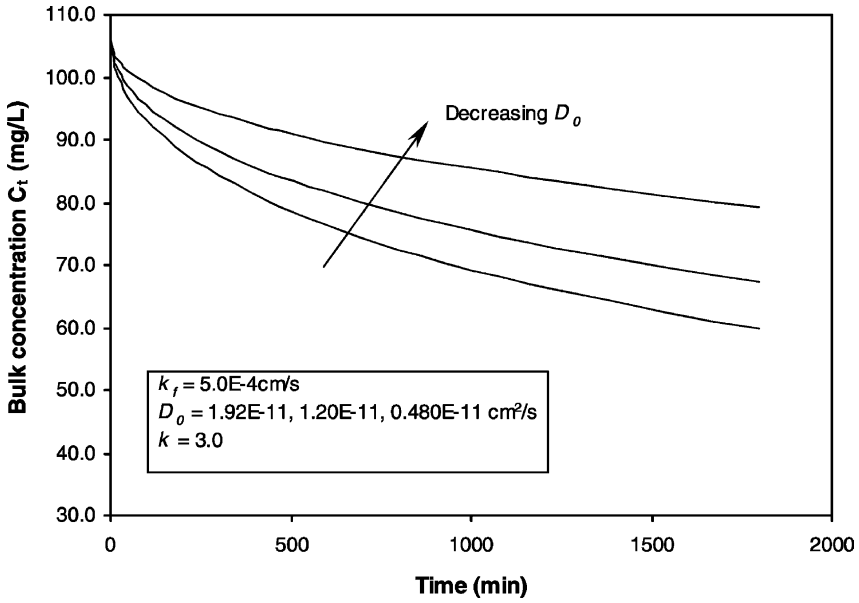

Fig. 5. Parametric sensitivity analysis; effect of D_0 on the concentration decay curves.

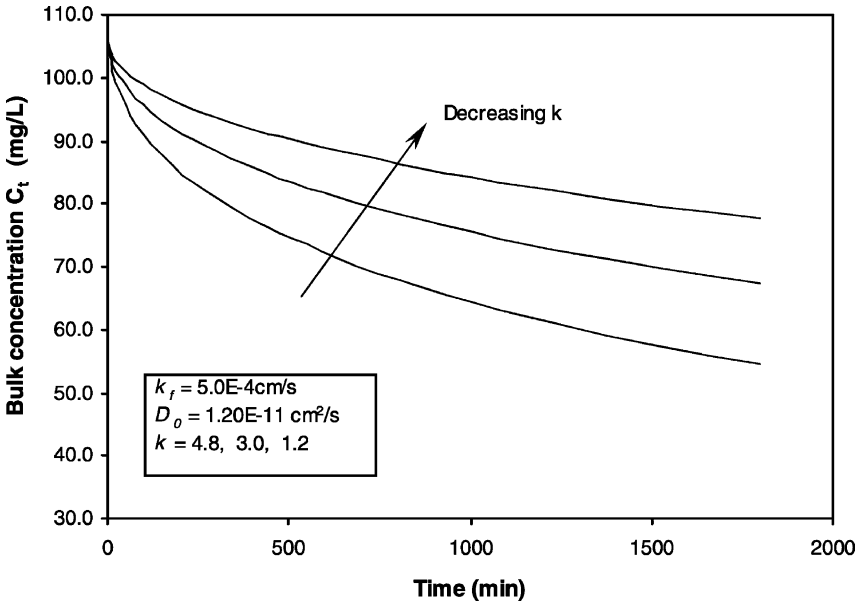

Fig. 6. Parametric sensitivity analysis; effect of k on the concentration decay curves.

Figs. 4–6 show that, increasing or decreasing k_f by up to 60% failed to bring noticeable change in the concentration decay curve, while it shows high sensitivity towards the same percentage changes in D_0 and k. The following conclusions can be drawn from this observation: (i) between the film diffusion and the surface diffusion, the latter is the rate-controlling step during adsorption; (ii) the accuracy of the best-fit k_f value by curve fitting is not very high. However, as can be seen from Table 1, the best-fit k_f value (5.0E−4 cm/s) has the same order of magnitude as those estimated from the initial slope method. This implies that the best-fit k_f value by curve fitting is physically plausible and thus acceptable. A more accurate k_f value should be obtained from an independent experiment for the investigated system; (iii) the high sensitivity of the concentration decay curve towards D_0 and k implies that the accuracy of the best-fit D_0 and k values is high. It also indicates that there is a strong interdependency between D_0 and k, because they have to be selected simultaneously in order to obtain the best-fitting curve. This is understandable, as can be seen from Eqs. (3) and (4), that D_0 and k are related via ϕ and ΔH_0 at a specific temperature T.

6. Conclusions

The film-solid diffusion model incorporating a concentration-dependent surface diffusivity represented by Eq. (2) was solved numerically with a finite-difference scheme. It could provide theoretical concentration decay curves for both the variant surface diffusivity model ($k \neq 0$) and the constant surface diffusivity model ($k = 0$).

The use of the film-solid diffusion model together with the concentration-dependent surface diffusivity has been found to give satisfactory predictions for the reactive dye/F-400 adsorption system. The intraparticle mass transfer coefficients (D_0 and k) obtained for such a system indicated a strong dependence of D_s on q. The present study has provided further validity of the concentration dependence of D_s represented by Eq. (2).

Parametric sensitivity analysis showed that the adsorption kinetic curve was very sensitive towards the intraparticle diffusion parameters D_0 and k, demonstrating that the intraparticle diffusion is the rate-controlling step during adsorption.

Acknowledgements

The authors would like to thank the board of CVCP and the School of Chemical Engineering, University of Birmingham for their financial support.

References

[1] A.P. Mathews, W.J. Weber Jr., Effects of external mass transfer and intraparticle diffusion on adsorption in slurry reactors, AIChE. Symp. Ser. 73 (1976) 91–98.
[2] H. Moon, W.K. Lee, Intraparticle diffusion in liquid-phase adsorption of phenols with activated carbon in finite batch adsorber, J. Colloid Interface Sci. 96 (1983) 162–171.
[3] B. Al-Duri, G. McKay, Prediction of binary system for kinetics of batch adsorption using basic dyes onto activated carbon, Chem. Eng. Sci. 46 (1991) 193–204.
[4] Y. Sudo, D.M. Misic, M. Suzuki, Concentration dependence of effective surface diffusion coefficients in aqueous phase adsorption on activated carbon, Chem. Eng. Sci. 33 (1978) 1287–1290.
[5] A. Kapoor, R.T. Yang, C. Wong, Surface-diffusion, Catal. Rev. 31 (1989) 129–214.

[6] K. Miyabe, S. Takeuchi, Model for surface diffusion in liquid-phase adsorption, AIChE J. 43 (1997) 2997–3006.
[7] E.R. Gilliland, R.F. Baddour, G.P. Perkinson, K.J. Sladek, Diffusion on surfaces. I. Effect of concentration on the diffusivity of physically adsorbed gases, Ind. Eng. Chem. Fundam. 13 (1974) 95–99.
[8] I. Neretnieks, Analysis of Some adsorption experiments with activated carbon, Chem. Eng. Sci. 31 (1976) 1029–1035.
[9] K. Higashi, H. Ito, J. Oishi, Surface diffusion phenomena in gaseous diffusion. I. Surface diffusion of pure gas, J. At. Energy Soc. Jpn. 5 (1963) 846.
[10] A. Kapoor, R.T. Yang, Contribution of concentration-dependent surface diffusion to rate of adsorption, Chem. Eng. Sci. 46 (1991) 1995–2002.
[11] X. Hu, S. Qiao, X.S. Zhao, G.Q. Lu, Adsorption study of benzene in ink-bottle-like MCM-41, Ind. Eng. Chem. Res. 40 (2001) 862–867.
[12] R. Gutsche, H. Yoshida, Solid diffusion in the pores of cellulose membrane, Chem. Eng. Sci. 49 (1994) 179–188.
[13] H. Komiyama, J.M. Smith, Surface diffusion in liquid-filled pores, AIChE J. 20 (1974) 1110–1117.
[14] D. Chatzopoulos, A. Varma, R.L. Irvine, Activated carbon adsorption and desorption of toluene in the aqueous phase, AIChE J. 39 (1993) 2027–2041.
[15] A. Reife, H.S. Freeman (Eds.), Environmental Chemistry of Dyes and Pigments, Wiley/Interscience, New York, 1996.
[16] B.A. Finlayson, Nonlinear Analysis in Chemical Engineering, McGraw-Hill, New York, 1980.
[17] R.G. Peel, A. Benedek, C.M. Crowe, A branched pore kinetic model for activated carbon adsorption, AIChE J. 27 (1981) 26–32.
[18] X. Yang, B. Al-Duri, Application of branched pore diffusion model in the adsorption of reactive dyes on activated carbon, Chem. Eng. J. 83 (2001) 15–23.
[19] P. Cooper (Ed.), Colour in Dyehouse Effluent, Alden Press, Oxford, UK, 1995.
[20] H. Spahn, E.U. Schlünder, The scale-up of activated carbon columns for water purification, based on results from batch tests. I. Theoretical and experimental determination of adsorption rates of single organic solutes in batch tests, Chem. Eng. Sci. 30 (1975) 529–537.
[21] M. Miyahara, M. Okazaki, Concentration dependence of surface diffusivity of nitrobenzene and benzonitrile in liquid-phase adsorption onto an activated carbon, J. Chem. Eng. Jpn. 25 (1992) 408–414.
[22] J.M. Smith, H.C. van Ness, M.M. Abbott, Introduction to Chemical Engineering Thermodynamics, McGraw-Hill, London, 1996.